IEEE Access
Multidisciplinary ⋮ Rapid Review ⋮ Open Access Journal

Received December 23, 2020, accepted January 6, 2021, date of publication January 12, 2021, date of current version January 25, 2021.

Digital Object Identifier 10.1109/ACCESS.2021.3050876

Numerical Modeling, Electrical Characteristics Analysis and Experimental Validation of Severe Inter-Turn Short Circuit Fault Conditions on Stator Winding in DFIG of Wind Turbines

YU CHEN[1], (Senior Member, IEEE), ATTIQ UR REHMAN[1], (Student Member, IEEE), YIHAN ZHAO[1], LULU WANG[1], SHUANG WANG [1], (Member, IEEE), MIN ZHANG[2], (Member, IEEE), YONG ZHAO[3], YONGHONG CHENG[1], (Senior Member, IEEE), AND TOSHIKATSU TANAKA[4], (Life Fellow, IEEE)

[1]School of Electrical Engineering, Xi'an Jiaotong University, Xi'an 710049, China
[2]School of Mathematics, Northwest University, Xi'an 710049, China
[3]Xi'an Thermal Power Research Institute Company Ltd., Xi'an 710032, China
[4]IPS Research Center, Waseda University, Kitakyushu 808-0135, Japan

Corresponding author: Yu Chen (chenyu@xjtu.edu.cn)

This work was supported by the Headquarters Science and Technology Projects of China Huaneng Group under Project HNKJ18-H32.

ABSTRACT Inter-turn short circuit fault (ITSCF) can be a great threat for the safety and effectiveness of the generator. In this paper, a simulation model with the experimental platform is established to diagnose the ITSCF in stator windings. A simulation model based on the Finite Element Method (FEM) is designed in ANSYS. Stator current is used for calculating the Root-Mean-Square (RMS) value, phase difference, symmetrical components, Park's vector trajectory's and Total Harmonic Distortion (THD). It was found that when ITSCF happened, three phase currents in stator is no longer symmetrical. The ratio of negative to positive sequence of current raises from 0.40 to 14.18 in simulation and 0.52 to 19.89 in the experiment from normal condition to 7 turns shorted. The same trend was seen in Park's vector trajectory analysis where the eccentricity raises from 0.03 to 0.65 in simulation and 0.14 to 0.75 in the experiment. Phase difference of the three phases is at 120° degree deviation as the ITSCF occurs in stator winding. THD also increased with the increase in the fault level. The results show a good consistency of simulation with experimental results. It was found that the analysis performed in this research are major indications for serious fault in DFIG.

INDEX TERMS Fault diagnosis, finite element methods, induction machines, numerical analysis.

I. INTRODUCTION

Power generation through wind is one of the most auspicious source of renewable energy, which is getting massive attention from the last few decades because of environment pollution and energy crisis in many countries [1]–[3]. According to the 2018 Global Wind Energy Council's report, the global wind power installed capacity has arisen to 591 GW and the newly developed is 51.3 GW [4]. Doubly-Fed Induction Generator (DFIG) has the advantages of high efficiency, low investment, variable power factor and small capacity of frequency conversion device from other generators so that it is broadly used in wind power industry [2], [5].

Normally wind farms are located in poor-environment and remote areas and are usually installed at a distance of 50 to 80 meters above the ground. All these features put difficulties in maintenance work and increase maintenance costs. The report of Electric Power Research Institute pointed out that 47% of DFIG failures are allied to bearings faults, 10% are rotor windings faults and 37% of machine failure is because of stator related faults [6], [7]. From these 37% stator faults most faults are linked with stator windings faults and are initiated from inter-turn short-circuit fault (ITSCF). When ITSCF occurs, the temperature and current increases which in turn results in more serious faults, for example, phase-to-phase or

The associate editor coordinating the review of this manuscript and approving it for publication was Hao Luo.

phase-to-ground short-circuit faults [8]–[11]. Therefore, it is important to detect the potential failures that could reduce the losses.

Simulations and experiments are two ways to study DFIG faults. Simulation modelling has attracted much attention because of the advantages of safety, economic and speediness. It uses the parameters of actual DFIG to establish the model in software. So far, the mainly used simulation methods are Coordinate Method (CM), Equivalent Circuit Method (ECM), Equivalent Magnetic Circuit Method (EMCM), Multi-Loop Method (MLM), Finite Element Method (FEM), etc. The software ranges from MATLAB, ANSYS and so on [12]–[14].

However, a simulation model is a simplification of real generators, which can't represent the generator's actual condition, so an experimental study is necessary [15], [16]. Stefani A. built a 3.3kW doubly fed induction generator and experiment about the unbalanced fault [17]. They set resistance in rotor and stator phase to simulate faults. Simon Jonathan Watson set up an 11kW doubly fed generator fault platform, which can simulate stator short-circuit fault, rotor unbalance fault and mechanical fault [18]. Especially, rotor and stator faults are realized by external resistance. Q.F. Lu applies a paralleled resistance in the stator phase to implement a stator winding fault [19]. Hongzhong Ma establishes a 5.5kW doubly fed induction generator that can merely achieve a small number of turns ITSCF [20]. In fact, most of the experimental setup was designed for the lower rated power of the machine in wind farms, so it is essential to establish a high-power generator to study the stator ITSCF.

Many data associated with condition monitoring has been surveyed which was used for different purposes, like practical approaches regarding condition monitoring [21], or other technical problems associated with them [22]. The condition monitoring systems will prepare a fault detection system that will detect the fault at its initial stage and will result in removing or decreasing the costs of unexpected and unscheduled repairing. There are several condition monitoring systems which are based on torque, acoustic, temperature, oil, vibration and electrical signals. Through all of them, the electrical signal monitoring is usually used, which comprises flux, voltage, power and current monitoring. The current monitoring method is widely used as the current sensors used in the experiment are cheap and easy to install [23]. In this paper, five different analysis methods were applied to stator three phase currents to detect the stator ITSCF at its initial stage. These analysis methods present a potential breakthrough with its ability to detect the ITSCF in the stator winding at its initial stage and also determine the fault severity.

The paper is structured as follows. Section II describes the fault simulation modelling. Section III presents the experimental setup and fault introduction in the stator winding. Result analysis and fault features extraction are discussed in Section IV. In the end, conclusions are explained in Section V.

In this paper study of FEM simulation and experiment of stator ITSCF in DFIG was carried out. Simulation and experimental results are analyzed to extract fault features. The simulation results are proved by experimental tests.

II. SIMULATION MODELLING

A. FEM METHOD

FEM is a numerical method which is established on variation principles. It solves the partial differential equation and integral equation and provides more precise information than any other analyses method. In this technique, the magnetic linearized parameters are used to solve the problem.

A two-dimensional electromagnetic field-circuit coupled model of DFIG was designed by the vector magnetic potential Az. In this simulation technique, the whole generator is reflected as a calculating field for the study of ITSCF in the stator winding. The electromagnetic field equation of electrical machines is shown in (1).

$$\begin{cases} \dfrac{\partial}{\partial x}\left(\mu\dfrac{\partial A_Z}{\partial x}\right)+\dfrac{\partial}{\partial y}\left(\mu\dfrac{\partial A_Z}{\partial y}\right) \\ \qquad = -J_Z+\sigma\dfrac{\partial A_Z}{\partial t}+v_x\sigma\dfrac{\partial A_Z}{\partial x} \\ A_Z|_{\Gamma_1}=A_{Z0} \\ \left.\dfrac{1}{\mu}\dfrac{\partial A_Z}{\partial n}\right|_{\Gamma_2}=-H_t \end{cases} \tag{1}$$

In (1), JZ is z component of the source current, vx is x component of rotational speed, σ is conductivity, μ is permeability, AZ0 is the given value of AZ on the boundary of $\Gamma 1$ and $\Gamma 2$ is the Neumann Boundary Condition.

B. STATOR FAULT MODEL IN ANSYS

Generally, there are different ways to establish a DFIG geometrical model. The more accurate and simplest technique is to build the geometrical model in ANSYS/RMxprt software and then import this geometrical model into Maxwell 2D for further analysis. The geometrical model of the DFIG for the normal condition is shown in Fig. 1.

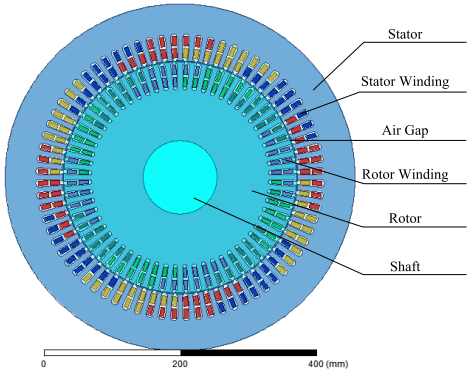

FIGURE 1. Geometrical model of DFIG for normal condition.

ITSCF is a type of fault and is hard to identify at the initial stage. It can lead to more serious faults, for example, phase-to-phase short-circuit and phase-to-ground short-circuit fault and can bring the huge losses and even destroy the machine if its didn't detect at the initial stage of the fault.

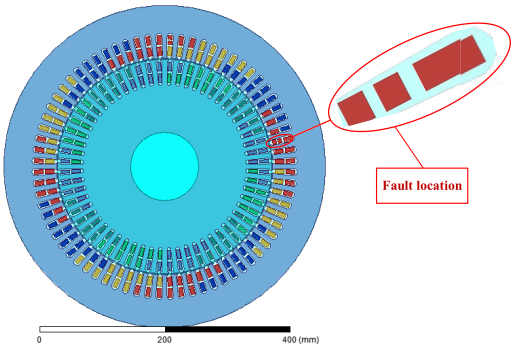

FIGURE 2. Geometrical model of ITSCF.

Each phase of the stator has four branches which are parallel to each other. Two kinds of ITSCF can happen in the machine: 1) fault happened in the same branch; 2) fault happened in two different branches. In this paper, a fault occurred in the same branch will be discussed because the latter is much more serious and obvious than the former.

In the simulation model, the stator has four branches in each branch A1 then this (branch A1) will be further divided into three parts: one short-circuited winding A1_sc and the other two are non-short-circuited windings A1_1 and A1_3. The short-circuit fault in phase A is achieved when the switch is closed. If the ITSCF is located in the third coil of the same phase. In the same way, different turns short-circuit fault can be achieved.

External circuit model was used to provide the excitation to stator windings in this simulation which take end leakage-inductances of stator windings into consideration. Rotor windings provide the three-phase AC source. The geometrical model of phase A of the stator winding ITSCF is shown in Fig. 2. The field-circuit coupling technique is used to establish the model. Additionally, the end-effect of the generator is considered, the end leakage-inductance L and terminal resistance R for different short-circuited turns are calculated in the external circuit.

III. EXPERIMENTAL SETUP AND FAULT INTRODUCTION IN STATOR WINDING

A. EXPERIMENTAL SETUP

Doubly fed induction generator (100 kW), converter, drive motor, data acquisition system, control system and short-circuit cabinet were the main components in this experiment. The whole experiment system of DFIG is presented in Fig. 3. Control system was used for the starting of the motor, speed regulation and temperature display. The key task of the short circuit cabinet was to perform different levels of ITSCF by 14 programmable controllers. Data storage recorder (HIOKO 8860) and current transformers were used as data acquisition devices. The important parameters of the DFIG used in the experiment are given in Table 1.

B. FAULT INTRODUCTION IN STATOR WINDINGS

In the experimental setup, at least three taps can be extracted from each slot because of the limit of slot space, which is considered in the design stage. There were eight outgoing wires which were fixed with stator coils. These outgoing wires were coupled to different switches in the short-circuit cabinet to perform the ITSCFs. Outgoing wires are labelled from node 1 to node 8, thus two to eight turns short-circuit can be accomplished by shutting off these switches. These ITSCFs are made both in the simulation model and in an experimental setup in the same way.

Each tap was connected with suitable resistance to protect the generator during ITSCF tests. The resistor was used to limit the current flowing in the inter-turn loop. During the experiment, from 0.07Ω to 2.6Ω resistor were used for the test. And we found that if we experiment without a resistor, there was more chance that some serious fault could happen as the circulating current was high. Then we used 0.07Ω and got good results. When we use a higher resistor than 0.07Ω then the results were not good. That's why in this experiment 0.07Ω were used. The experimental setup is presented in Fig. 4.

TABLE 1. Generator's parameters.

Parameter	Value (Stator/Rotor)	Parameter	Value (Stator/Rotor)
Rated output power	100 kW	Rated speed	1800 rpm
Circuit type	△/Y	Inner diameter	346.4/110 mm
Outer diameter	520/350 mm	Winding layers	2/2
Number of turns per phase	72/60	Number of slots	228/100
Length	290 mm	Coil pitch	15/13
Number of poles	4	Conductors per slot	19/10
Parallel branches	4/1	Rated power factor	1
Rated voltage	380 V	Frequency	50 Hz

IV. RESULT ANALYSIS AND FAULT FEATURE EXTRACTION

A 100 kW wound rotor induction generator is used for the simulation model and experimental setup. In this research, two-seven turns short-circuit faults were performed. Stator currents were acquired to analyze the RMS, sequence current analysis, the eccentricity of the park's vector trajectory, phase difference, and Total Harmonics Distortion.

A. TIME DOMAIN ANALYSIS

Three phase currents of simulation and experiment for stator winding in healthy condition is presented in Fig. 5. When the machine is operating normally all the three phase currents are symmetrical. Fig. 6 and Fig. 7 display the simulation and experiment results when there 2 to 7 turns' short-circuit faults. These figures show that when there is a fault in the generator the three phase currents are no longer symmetrical. This asymmetrical behaviour is clear as the number of shorted turns increases. In Table 2, the RMS values for healthy and ITSCF is given. The result shows that in healthy condition all the three phases have almost same value of current, but in

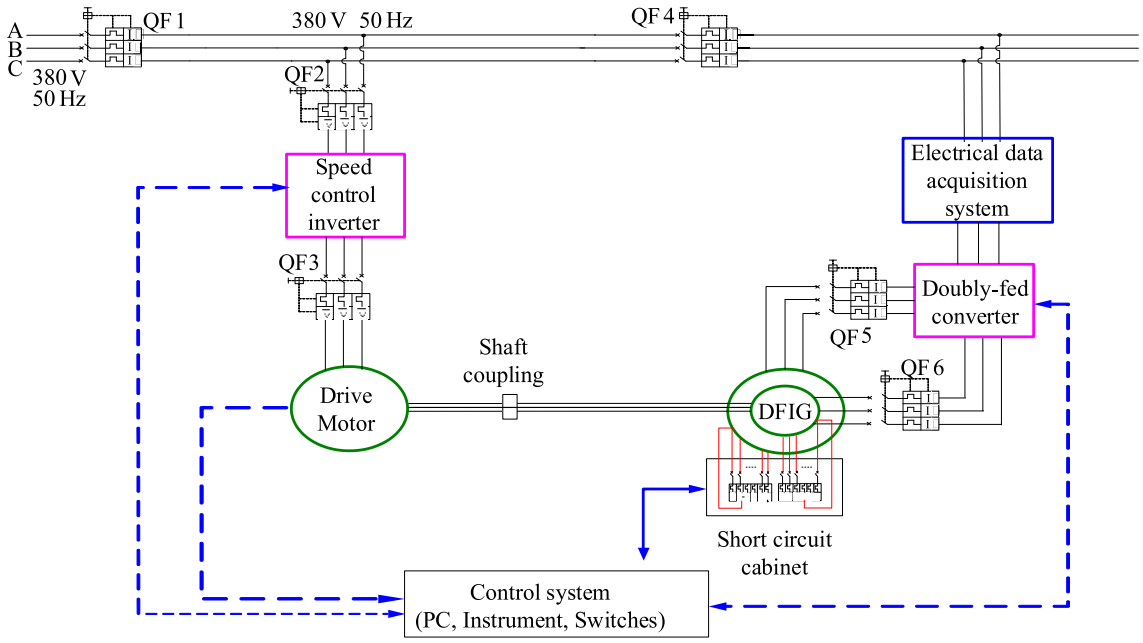

FIGURE 3. Experimental setup of DFIG for ITSCF in stator windings.

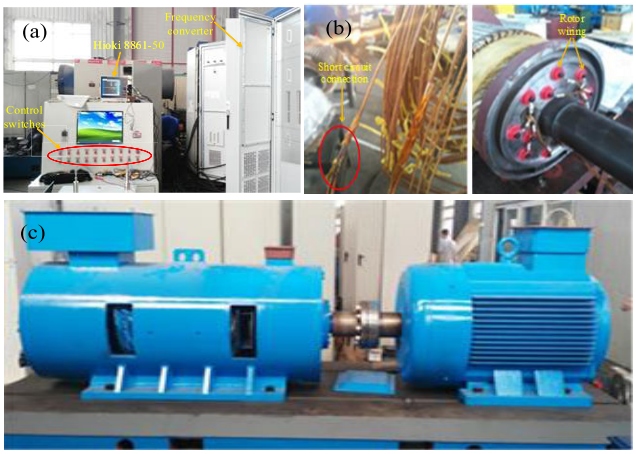

FIGURE 4. Experimental setup. (a) Frequency converter and control system, (b) Tapping points and rotor wiring, (c) Drive motor and induction generator.

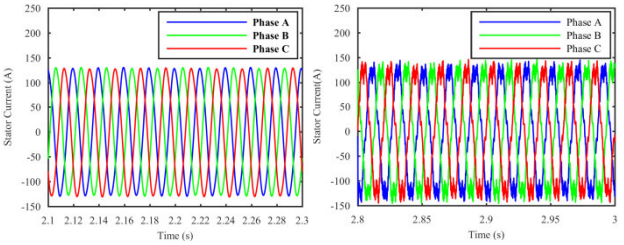

(a) Healthy condition (Simulation) (b) Healthy condition (Experiment)

FIGURE 5. Stator currents under healthy condition.

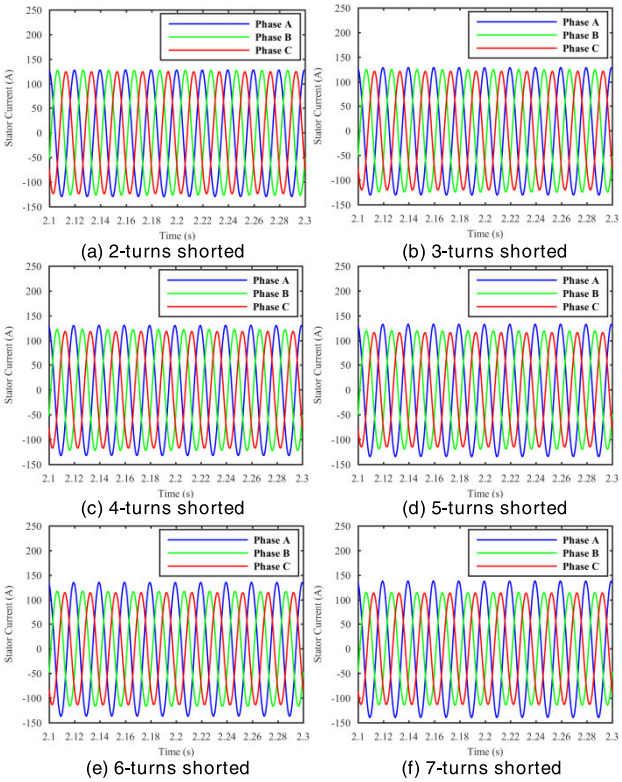

(a) 2-turns shorted (b) 3-turns shorted (c) 4-turns shorted (d) 5-turns shorted (e) 6-turns shorted (f) 7-turns shorted

FIGURE 6. Stator currents under 2, 3, 4, 5, 6 and 7 turns short circuited fault (Simulation).

faulty condition, phase A has a higher value than phase B and phase C. As the fault becomes severe, the difference of the amplitude of three phases also increases. Therefore, form the amplitude difference, the level of the fault can be estimated.

B. SYMMETRICAL COMPONENT METHOD

According to the method of symmetrical components, three-phase currents $\dot{I}_A, \dot{I}_B$ and $\dot{I}_C$ decomposed into the positive sequence current, negative sequence current and zero

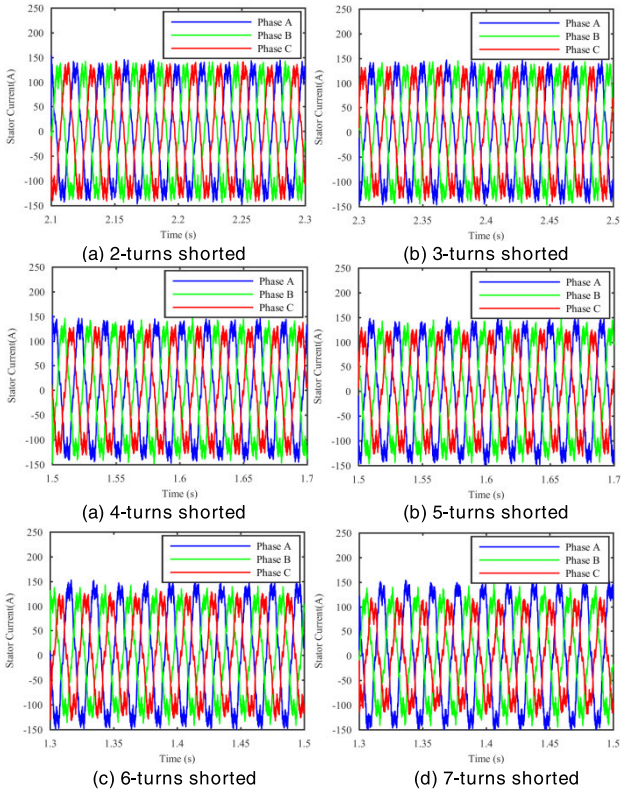

FIGURE 7. Stator currents under 2, 3, 4, 5, 6 and 7 turns short circuited fault (Experiment).

TABLE 2. RMS values under different number of shorted turns.

Shorted turns	Simulation			Experiment		
	A	B	C	A	B	C
0	90.79	90.83	91.47	91.42	92.21	91.36
2	91.26	90.11	87.60	91.92	90.51	89.31
3	91.91	88.52	85.08	93.17	90.58	86.50
4	93.08	86.70	82.95	94.78	89.49	83.62
5	94.61	84.85	81.39	96.96	88.54	80.80
6	96.38	83.15	80.41	98.72	82.92	80.53
7	98.28	81.42	79.98	100.69	83.99	72.95

sequence current.

$$\begin{cases} \dot{I}_1 = \dfrac{1}{3}\left(\dot{I}_A + a\dot{I}_B + a^2\dot{I}_C\right) \\ \dot{I}_2 = \dfrac{1}{3}\left(\dot{I}_A + a^2\dot{I}_B + a\dot{I}_C\right) \\ \dot{I}_0 = \dfrac{1}{3}\left(\dot{I}_A + \dot{I}_B + \dot{I}_C\right) \end{cases} \tag{2}$$

In (2), $a = 1\angle 120° = e^{j120°}$.

Each sequence current can be calculated through three-phase currents. However, they are complicated to get.

Although the sequence current can be calculated from the instantaneous value of three-phase currents, the calculation process is complex. The connection of the generator's stator winding and the power grid is a three-phase three-wire system, so the neutral point is not grounding. Sum of three-phase currents is equal to zero for the inexistence of zero sequence current presented in (3).

Suppose $\dot{I}_A = I_A e^{j0}$, $\dot{I}_B = I_B e^{j\varphi_b}$ and $\dot{I}_C = I_C e^{j\varphi_c}$. Presume $I_B = xI_A$, $I_C = yI_A$.

$$\dot{I}_A + \dot{I}_B + \dot{I}_C = 0 \tag{3}$$

$$\begin{cases} \cos\alpha_1 = \dfrac{I_B^2 + I_c^2 - I_A^2}{2I_B I_c} = \dfrac{x^2 + y^2 - 1}{2xy} \\ \cos\alpha_2 = \dfrac{I_A^2 + I_c^2 - I_B^2}{2I_A I_c} = \dfrac{1 + y^2 - x^2}{2y} \\ \cos\alpha_3 = \dfrac{I_A^2 + I_B^2 - I_c^2}{2I_A I_B} = \dfrac{1 + x^2 - y^2}{2x} \end{cases} \tag{4}$$

$$\frac{\sin\alpha_1}{I_A} = \frac{\sin\alpha_2}{I_B} = \frac{\sin\alpha_3}{I_C} \tag{5}$$

According to sine and cosine theorem, (4) and (5) can be obtained and according to the basic theorem of a trigonometric function, it can deduce the expression for the positive sequence of current and negative sequence of current, shown in (6) and (7).

$$\begin{cases} I_{1x} = \dfrac{I_A}{2}\left\{1 + \dfrac{1}{\sqrt{3}}\sqrt{\left[(x+y)^2 - 1\right]\left[(1+y)^2 - x^2\right]}\right\} \\ I_{1y} = \dfrac{I_A}{2\sqrt{3}}\left(y^2 - x^2\right) \end{cases} \tag{6}$$

$$\begin{cases} I_{2x} = \dfrac{I_A}{2}\left\{1 - \dfrac{1}{\sqrt{3}}\sqrt{\left[(x+y)^2 - 1\right]\left[(1+y)^2 - x^2\right]}\right\} \\ I_{2y} = \dfrac{I_A}{2\sqrt{3}}\left(x^2 - y^2\right) \end{cases} \tag{7}$$

The sequence component analysis indicates the generator behaviour. Three phase stator currents were taken to calculate the sequence components. The results of positive, negative and ratio of negative and positive current for simulation and experiment are given in Table 3. Which can be used as a fault feature parameter. Both in simulation and experiment, normal and two to seven turns short-circuit faults are conducted. When the generator is operating in normal condition then three phase current will have only a positive sequence of current. From the obtained results, it was observed that the stator three phase current have some small value of the negative sequence of current which is negligible.

TABLE 3. Symmetrical component analysis under different number of shorted turns.

Shorted turns	Simulation			Experiment		
	I_1	I_2	I_2/I_1 (%)	I_1	I_2	I_2/I_1 (%)
0	91.28	0.34	0.37	91.66	0.48	0.52
2	89.64	2.15	2.40	90.58	1.49	1.64
3	88.46	3.95	4.47	90.04	3.87	4.30
4	87.47	5.97	6.82	89.18	6.48	7.27
5	86.76	8.07	9.30	88.51	9.50	10.73
6	86.33	10.15	11.76	86.93	12.05	13.86
7	86.09	12.21	14.18	84.96	16.90	19.89

Under the faulty condition, the generator shows asymmetrical behaviour and have negative-sequence current in it and that negative-sequence current increased with fault

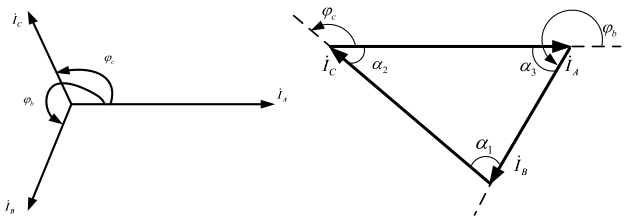

FIGURE 8. The diagram of stator three-phase currents.

degree. It is presented that the ratio of negative and positive currents increases with fault severity both in simulation and in the experiment. The simulation and experiment results have a little different because of the external disturbance in the experiment. The ratio is a little high in the experiment because the experimental result is affected by the noise and grid voltage. But for 2 and 3 turns, the amplitude of the simulation result is higher than the experimental result, which didn't have any effect on analysis. The comparative results of sequence currents of simulation and experiment for normal and at different ITSCF conditions are displayed in Fig. 9.

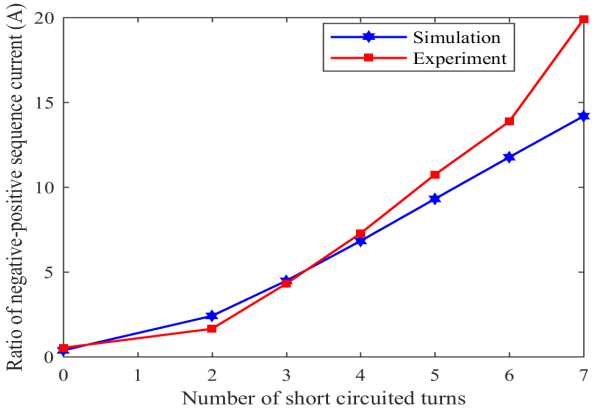

FIGURE 9. Comparison of ratio of sequence current.

The results show that if the value of negative-sequence current is low then the number of faulted turns are low, if the value of negative-sequence current is high then the number of shorted turns are high. Therefore, it can be concluded that the value of negative-sequence current depends on the fault severity. The same trend can be seen in the ratio of negative and positive currents analysis.

C. PARK VECTOR METHOD

Three phase currents can be easily converted from three phase axis into two-phase axis coordinate by the principle of magnetic potential balance. So, the vector $\dot{I} = i_\alpha + ji_\beta$ is called a park's vector and the transform equation is shown in (8). For normal condition, the Park's vector trajectory is in the form of a circle centred on the origin. But when ITSCF happened, it turns to be an ellipse.

$$\begin{cases} i_\alpha = \sqrt{\dfrac{2}{3}} i_A - \dfrac{1}{\sqrt{6}} i_B - \dfrac{1}{\sqrt{6}} i_C \\ i_\beta = \dfrac{1}{\sqrt{2}} i_B - \dfrac{1}{\sqrt{2}} i_C \end{cases} \tag{8}$$

Park's vector trajectory is only a qualitative analysis, further feature extraction is needed to represent fault severity. The general equation of ellipse can be got through Park's vector trajectory in (9).

$$Ax^2 + Bxy + Cy^2 + Dx + Ey + 1 = 0 \tag{9}$$

In (10) and (11), the geometric centre of the ellipse is (X_c, Y_c).

$$X_c = \frac{BE - 2CD}{4AC - B^2} \tag{10}$$

$$Y_c = \frac{BD - 2AE}{4AC - B^2} \tag{11}$$

Therefore, the length of the semi-minor and semi-major axis are shown as follows:

$$a = \sqrt{\frac{2(AX_c^2 + CY_c^2 + BX_cY_c - 1)}{A + C + \sqrt{(A-C)^2 + B^2}}} \tag{12}$$

$$b = \sqrt{\frac{2(AX_c^2 + CY_c^2 + BX_cY_c - 1)}{A + C - \sqrt{(A-C)^2 + B^2}}} \tag{13}$$

The eccentricity of park's vector trajectory is given in (14).

$$e = \frac{\sqrt{a^2 - b^2}}{a} \tag{14}$$

It is not useful to extract the long or short axis of the Park vector as a fault feature. For different running conditions, generators may have different axis length of the Park vector even they are in the same fault. The eccentricity is a better choice to be the fault feature parameter, which shows the unbalanced degree of stator ITSCF.

TABLE 4. Parks' vector under different number of shorted turns.

Shorted turns	Simulation			Experiment		
	Length of semi-major axis	Length of semi-minor axis	Eccentricity	Length of semi-major axis	Length of semi-minor axis	Eccentricity
0	158.15	158.07	0.03	158.18	156.62	0.14
2	158.60	151.93	0.29	157.58	153.11	0.24
3	159.70	146.72	0.39	160.50	148.23	0.38
4	161.50	141.49	0.48	163.87	142.31	0.50
5	163.85	136.63	0.55	168.64	135.69	0.59
6	166.54	132.42	0.61	169.68	129.02	0.65
7	169.55	128.54	0.65	175.81	116.81	0.75

The trajectory of park vector is in the form a circle when the machine is running normally but when ITSCF faults occur three-phase currents are unbalanced, park vector trajectory turns to an ellipse. The length of semi-major axis is increasing and the length of semi-minor axis is decreasing as the fault level is increasing which is shown in Table 4. From Fig. 10, it is shown that the Park vector of the stator current is a circle under normal condition. It turns into an ellipse when short-circuit fault occurs, which is shown in Fig. 11 and Fig. 12 for both simulation and experiment respectively. Both simulation and experimental results spectacle that the eccentricity gets larger with deeper fault degree.

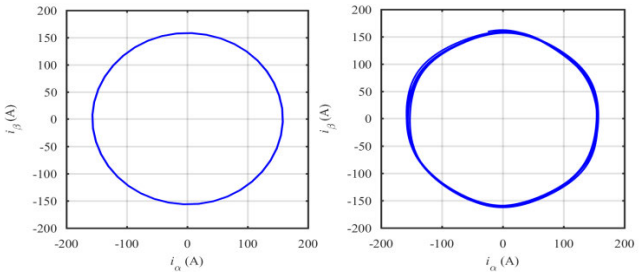

FIGURE 10. Park's vector trajectory under healthy conditions.

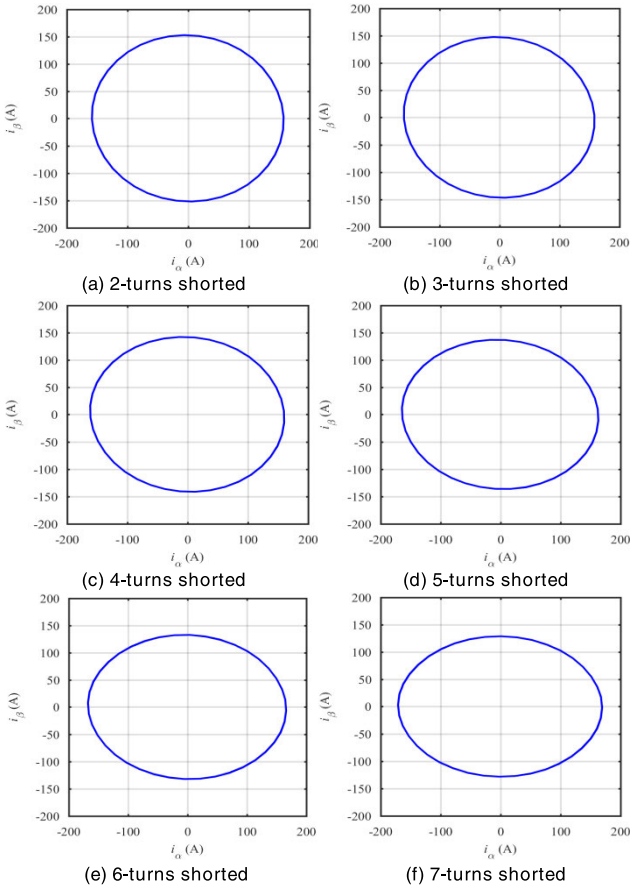

FIGURE 11. Park's vector trajectory under 2, 3, 4, 5, 6 and 7 turns short circuited fault (Simulation).

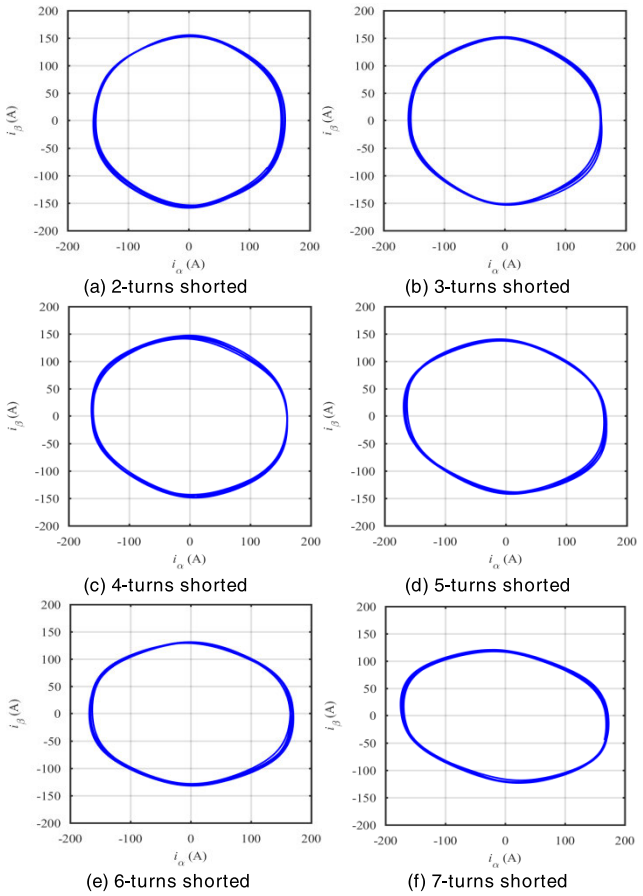

FIGURE 12. Park's vector under 2, 3, 4, 5, 6 and 7 turns short circuited fault (Experiment).

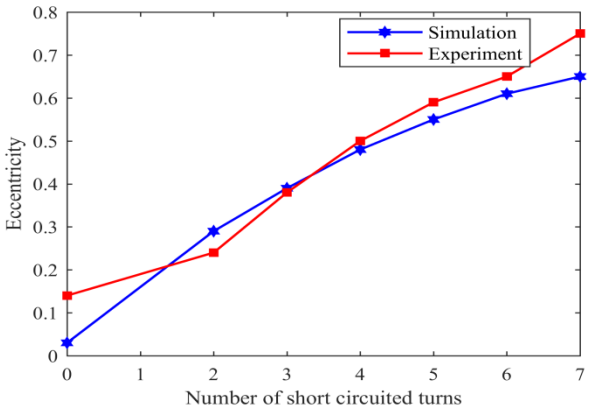

FIGURE 13. Comparison of eccentricity.

The shape of the eccentricity tells the fault severity, if the shape of the trajectory of park vector is closer to circle then it means that fewer turns i.e. 2 or 3 are shorted. If the shape of the trajectory of park vector is closer to ellipse then it means that more turns i.e. 6 or 7 are shorted which is shown in Fig. 11 and Fig. 12. Also from the value of the semi-major axis and the semi-minor axis, the severity of the fault can be calculated. The experimental result is a little high because of complicated experimental conditions. But for 2 and 3 turns, the amplitude of the simulation result is higher than the experimental result, which didn't have any effect on analysis. The comparative result of the eccentricity of simulation and experiment is presented in Fig. 13. The simulation and experimental results have a good agreement with each other.

D. PHASE DIFFERENCE ANALYSIS

In normal condition, there is a 120° phase difference between the two phases. But when short circuit occurred, the three phase currents are deviated from its position and are no longer

in the symmetrical form. From the phase difference of two phases, the severity of the fault can be measured. This was proved from the simulation and then validated experimentally in this research. The phase difference results of the stator current for simulation and experiment are specified in Table 5. During the normal operation of the machine all the three phases have phase difference of 120° from each other. When the fault occurred in the winding, the electrical angle deviates from 120°, and the faulty phase angle increases with fault level, which can be seen in Table 5. The phase difference of phases AB and CA is increasing as phase A is shorted phase and the phase difference of phases BC is decreasing because phase B and phase C are the non-faulty phases. The result shows that when there are lower turns shorted than the phase difference of the two phases are low and when the phase difference of the two phases are higher than it means that high turns are shorted. Both simulation and experiment results have the same trend for the phase difference analysis.

TABLE 5. Phase difference under different number of shorted turns.

Shorted turns	Simulation			Experiment		
	AB	BC	CA	AB	BC	CA
0	120.28	119.63	120.09	120.18	120.27	119.55
2	122.25	118.23	119.52	121.23	118.45	120.32
3	123.78	116.10	120.12	123.73	116.38	119.89
4	125.20	113.50	121.30	126.08	113.52	120.40
5	126.41	110.66	122.93	128.75	110.02	121.23
6	127.42	107.81	124.77	128.39	105.15	126.46
7	128.18	104.98	126.84	135.01	99.68	125.31

TABLE 6. Total harmonics distortion under different number of shorted turns.

Shorted turns	Simulation			Experiment		
	A%	B%	C%	A%	B%	C%
0	13.539	13.684	13.764	14.450	14.122	13.833
2	13.772	13.541	13.648	14.972	14.584	14.822
3	13.776	13.542	13.641	15.770	14.594	14.546
4	13.780	13.543	13.634	15.889	14.136	14.712
5	13.785	13.546	13.630	17.408	13.825	14.929
6	13.787	13.551	13.619	17.607	13.276	16.518
7	13.790	13.563	13.619	20.480	13.397	16.581

E. TOTAL HARMONICS DISTORTION (THD)

Total Harmonics Distortion (THD) for normal and 2 to 7 turns short circuit for simulation and experimental results are given in Table 6. From the results explained in table shows that the THD of the stator phase A current is affected when the ITSCF happened. The simulation result shows that during the healthy condition of the machine, it has 13.5386%, 13.6842% and 13.7643% of the THD for phase A, phase B and Phase C respectively. When the fault occurs the THD of the faulted phase (A) increases. During the 2 turns short circuited it has 13.7721% and finally reach to 13.79% for 7 turns short circuited. In the experiment, for the healthy condition of the machine, the THD has 14.45%, 14.1224% and 13.8333% for phase A, phase B and Phase C respectively. The THD of the faulty phase (A) increases. For 2 turns short circuit fault, the THD is 14.9718% and it grows to 20.4798% for 7 turns short circuit fault. It has been concluded that when the fault is more serious the THD will be bigger. The THD of faulty-phase is larger than the other two non-faulty phases. In the experiment, THD has a higher value as compared to simulation, due to noises and disturbances from the outside environment. So it has been suggested that the THD regarded as a feature for fault phase and fault degree.

V. CONCLUSION

In this paper, simulation and experimental works were done to find out a relationship of some specific parameters for ITSCF in DFIG. It was found that five major parameters such as time domain analysis, symmetrical component method, park vector method, phase difference analysis and total harmonics distortion (THD) analysis could be effective evidence to diagnose the ITSCF in stator windings. Based on the finite element model (using ANSYS Maxwell) stator windings ITSCF was established. An experimental setup was developed to validate the simulation results. Through simulation and experiment results, some fault feature parameters were extracted. These fault features are useful for the diagnosis of the ITSCF in stator windings. The following results were obtained:

(1) Based on simulation and experiment results, it was found that all the three phase currents are symmetrical when the machine is running in normal condition, and it will become asymmetrical when the ITSCF occurs.

(2) As a result of the symmetrical component method, it was found that the negative sequence of current increases with the level of fault, and the ratio of negative to positive component increased as the degree of fault increases.

(3) In park vector method, it was seen that the eccentricity has a small value and the length of semi-major axis and semi-minor axis are the same in normal condition. Eccentricity and the length of semi-major axis increases while the length of semi-minor axis decrease as the fault level increases.

(4) From the phase difference analysis, it was concluded that when the phase difference of the two phases are 120° from each other than the machine is running in normal condition. If the phase angle of the two phases deviates from 120°, it means that the machine has a fault. It was also observed that the phase difference of the faulty phase is higher than the non-faulty phases.

(5) In the last analysis, the THD was calculated. In THD it was found that when the ITSCF happened the THD increases. It was also found that the faulty phase will have the highest THD and as the fault level increases, the THD become bigger.

REFERENCES

[1] P. B. Eriksen, T. Ackermann, H. Abildgaard, P. Smith, W. Winter, and J. M. R. Garcia, "System operation with high wind penetration," *IEEE Power Energy Mag.*, vol. 3, no. 6, pp. 65–74, Nov. 2005.

[2] Y. Liu, Q. H. Wu, and X. X. Zhou, "Co-ordinated multiloop switching control of DFIG for resilience enhancement of wind power penetrated power systems," *IEEE Trans. Sustain. Energy*, vol. 7, no. 3, pp. 1089–1099, Jul. 2016.

[3] K. Xiahou, X. Lin, Y. Liu, and Q. H. Wu, "Robust rotor-current sensorless control of doubly fed induction generators," *IEEE Trans. Energy Convers.*, vol. 33, no. 2, pp. 897–899, Jun. 2018.

[4] K. Ohlenforst, S. Sawyer, A. Dutton, B. Backwell, R. Fiestas, J. Lee, L. Qiao, F. Zhao, and N. Balachandran. *Global Wind Report 2018*. Accessed: Feb. 20, 2020. [Online]. Available: https://gwec.net/wp-content/uploads/2019/04/GWEC-Global-Wind-Report-2018.pdf

[5] V. Gevorgian, Y. Zhang, and E. Ela, "Investigating the impacts of wind generation participation in interconnection frequency response," *IEEE Trans. Sustain. Energy*, vol. 6, no. 3, pp. 1004–1012, Jul. 2015.

[6] M. Malekpour, B. T. Phung, and E. Ambikairajah, "Modelling and diagnostic of incipient stator inter-turn short circuit fault in induction motors," in *Proc. IEEE Conf. Condition Monit. Diagnosis (CMD)*, Perth, WA, Australia, Sep. 2018, pp. 1–6.

[7] I. Tsyokhla, A. Griffo, and J. Wang, "Online condition monitoring for diagnosis and prognosis of insulation degradation of inverter-fed machines," *IEEE Trans. Ind. Electron.*, vol. 66, no. 10, pp. 8126–8135, Oct. 2019.

[8] F. Cheng, J. Wang, L. Qu, and W. Qiao, "Rotor-current-based fault diagnosis for DFIG wind turbine drivetrain gearboxes using frequency analysis and a deep classifier," *IEEE Trans. Ind. Appl.*, vol. 54, no. 2, pp. 1062–1071, Mar./Apr. 2018.

[9] N. Boumalha, R. Hachelef, D. Kouchih, M. Tadjine, and M. S. Boucherit, "Diagnostic and fault tolerant control by adaptive observer of doubly-fed induction generators with inter-turn rotor and stator fault based wind turbine," in *Proc. ICEE-B*, Boumerdes, Algeria, Oct. 2017, pp. 1–6.

[10] J. Q. Li, Y. Z. Ren, and D. Wang, "Multi-loop mathematical model and calculation of inductances in doubly fed induction generation," *Large Electr. Mach. Hydraulic Turbine*, vol. 6, pp. 5–10, Jun. 2013.

[11] J. Faiz and S. M. M. Moosavi, "Detection of mixed eccentricity fault in doubly-fed induction generator based on reactive power spectrum," *IET Electr. Power Appl.*, vol. 11, no. 6, pp. 1076–1084, Jul. 2017.

[12] D. C. Patel and M. C. Chandorkar, "Modeling and analysis of stator interturn fault location effects on induction machines," *IEEE Trans. Ind. Electron.*, vol. 61, no. 9, pp. 4552–4564, Sep. 2014.

[13] M. Eftekhari, M. Moallem, S. Sadri, and M.-F. Hsieh, "Online detection of induction motor's stator winding short-circuit faults," *IEEE Syst. J.*, vol. 8, no. 4, pp. 1272–1282, Dec. 2014.

[14] L. Fan, S. Yuvarajan, and R. Kavasseri, "Harmonic analysis of a DFIG for a wind energy conversion system," *IEEE Trans. Energy Convers.*, vol. 25, no. 1, pp. 181–190, Mar. 2010.

[15] P. Zhang, Y. Du, T. G. Habetler, and B. Lu, "A survey of condition monitoring and protection methods for medium-voltage induction motors," *IEEE Trans. Ind. Appl.*, vol. 47, no. 1, pp. 34–46, Feb. 2011.

[16] S. Grubic, J. M. Aller, B. Lu, and T. G. Habetler, "A survey on testing and monitoring methods for stator insulation systems of low-voltage induction machines focusing on turn insulation problems," *IEEE Trans. Ind. Electron.*, vol. 55, no. 12, pp. 4127–4136, Dec. 2008.

[17] A. Stefani, A. Yazidi, C. Rossi, F. Filippetti, D. Casadei, and G.-A. Capolino, "Doubly fed induction machines diagnosis based on signature analysis of rotor modulating signals," *IEEE Trans. Ind. Appl.*, vol. 44, no. 6, pp. 1711–1721, Dec. 2008.

[18] S. J. Watson, B. J. Xiang, W. Yang, P. J. Tavner, and C. J. Crabtree, "Condition monitoring of the power output of wind turbine generators using wavelets," *IEEE Trans. Energy Convers.*, vol. 25, no. 3, pp. 715–721, Sep. 2010.

[19] Q. F. Lu, Z. T. Cao, and E. Ritchie, "Model of stator inter-turn short circuit fault in doubly-fed induction generators for wind turbine," in *Proc. PESC*, Aachen, Germany, 2004, pp. 932–937.

[20] M. Hongzhong, Z. Zhiyan, and Z. Zhixin, "Research on DFIG stator winding inter-turn short circuit fault," *Electr. Mach. Control*, vol. 15, no. 11, pp. 50–54, 2011.

[21] Z. Hameed, S. H. Ahn, and Y. M. Cho, "Practical aspects of a condition monitoring system for a wind turbine with emphasis on its design, system architecture, testing and installation," *Renew. Energy*, vol. 35, no. 5, pp. 879–894, May 2010.

[22] G. M. J. Herbert, S. Iniyan, and D. Amutha, "A review of technical issues on the development of wind farms," *Renew. Sustain. Energy Rev.*, vol. 32, pp. 619–641, Apr. 2014.

[23] M. Blodt, P. Granjon, B. Raison, and G. Rostaing, "Models for bearing damage detection in induction motors using stator current monitoring," *IEEE Trans. Ind. Electron.*, vol. 55, no. 4, pp. 1813–1822, Apr. 2008, doi: 10.1109/TIE.2008.917108.

YU CHEN (Senior Member, IEEE) was born in Hebei, China, in 1977. He received the B.S., M.S., and Ph.D. degrees in electrical engineering from Xi'an Jiaotong University, China, in 2000, 2003, and 2008, respectively.

From 2008 to 2009, he was a Visiting Lecturer with the Graduate School of Information, Production and System, Waseda University, Japan. From 2009 to 2010, he was a Research Fellow with the Department of Electrical Engineering and Electronics, KIT, Japan. From 2010 to 2012, he was a Research Fellow with the Laboratory of Spacecraft Engineering Interaction Engineering, KIT. Since 2012, he has been an Associate Professor with Xi'an Jiaotong University. His research interests include on-line monitoring and diagnosis on power equipment, nanocomposite, and spacecraft charging.

ATTIQ UR REHMAN (Student Member, IEEE) was born in Punjab, Pakistan, in 1988. He received the B.S. degree in electronics engineering from the COMSATS Institute of Technology, Abbottabad, Pakistan, in 2010, and the M.S. degree in electrical engineering from Xi'an Jiaotong University, Xi'an, China, in 2015, where he is currently pursuing the Ph.D. degree in electrical engineering.

His research interests include motor design, fault diagnosis, and on-line monitoring of the motor.

YIHAN ZHAO was born in Shaanxi, China, in 1993. He received the B.S. degree in electrical engineering from the Wuhan University of Technology, Wuhan, China, in 2015. He is currently pursuing the Ph.D. degree in software engineering from Xi'an Jiaotong University, Xi'an, China.

His current research interests include condition monitoring and diagnostics of electrical machines.

LULU WANG was born in Henan, China, in 1991. She received the B.S. degree in electrical engineering from the Wuhan University of Technology, Wuhan, China, in 2013, and the M.S. degree in instrument science and technology from Xi'an Jiaotong University, Xi'an, China, in 2016.

She is currently a Junior Engineer with Envision Energy Company Ltd., Shanghai, China. Her current research interests include fault detection and condition monitoring of the electrical machine and drives.

SHUANG WANG (Member, IEEE) received the B.S. degree in electrical engineering from Xi'an Jiaotong University, China, in 2014, and the Ph.D. degree from The Hong Kong University of Science and Technology, in 2018.

Since 2018, she has been a Researcher with Xi'an Jiaotong University. Her research interests include dielectrics and metamaterials.

MIN ZHANG (Member, IEEE) was born in Shaanxi, China, in 1980. She received the B.S. and Ph.D. degrees from Xi'an Jiaotong University, China, in 2002 and 2010, respectively.

From 2011 to 2014, she was a Research Fellow with Gifu University, Japan. From 2014 to 2015, she was a Research Fellow with Kyoto University, Japan. Since 2016, she has been a Lecturer with Northwest University, China. Her research interest includes signal processing.

YONG ZHAO was born in Shanxi, China, in 1978. He received the B.S. and M.S. degrees in electrical engineering from Xi'an Jiaotong University, China, in 1999 and 2005, respectively.

He is currently a Senior Engineer with Xi'an Thermal Power Research Institute Company Ltd. His current fields of interests include electrical and new energy equipment testing technology.

YONGHONG CHENG (Senior Member, IEEE) was born in Anhui, China, in 1965. He received the M.S. and Ph.D. degrees in electrical engineering from Xi'an Jiaotong University, Xi'an, China, in 1991 and 1999, respectively.

Since 2001, he has been a Professor with Xi'an Jiaotong University. His research interests include the property of dielectric materials, failure mechanism of insulating materials under extreme conditions, aging mechanism of insulation in power equipment, online detecting, and diagnosis technique on electrical insulation.

Dr. Cheng is a member of the General Test Special Committee, General Armament Department of China, and the Committee of ETSC of China Electro-technical Society. He was awarded several research prizes in China. He was also awarded the Chang Jiang Scholar Professor, in 2009.

TOSHIKATSU TANAKA (Life Fellow, IEEE) received the Ph.D. degree from Osaka University.

He worked with CRIEPI for 38 years, and temporarily with Salford University, U.K., the Rennselaer Polytechnic Institute, General Electric, USA, and Kyushu University, Japan. He is currently a Professor with the IPS Graduate School, Waseda University. His special fields of research interests include electrical properties of polymers, insulation diagnostics, polymer nanocomposites, and dielectric failure and aging mechanisms of polymers, as well as laser-induced lightning, superconducting technologies, energy storage in electric power systems, fuel cells, and lithium secondary batteries.

Dr. Tanaka is a Life Fellow of IEEJ. He is also actively involved in IEEJ and CIGRE. He was a recipient of the Ministry of Science and Technology Prize, in 2000, the IEEJ Technology Progress Award, in 1988, the IEEE Whitehead Memorial Lecture Award, in 2001, and the IEEE Dakin Award, in 2002. He is a Distinguished Member of CIGRE.